Piezomagnetic behavior of Co-doped ZnO nanoribbons

R. H. Miwa,[1,*] T. M. Schmidt,[1] and A. Fazzio[2]
[1]*Instituto de Física, Universidade Federal de Uberlândia, Uberlândia, MG, Brazil*
[2]*Instituto de Física, Universidade de São Paulo, São Paulo, SP, Brazil*
(Received 12 March 2011; revised manuscript received 23 August 2011; published 14 October 2011)

Using *ab initio* total energy calculations, we show that bilayer systems of ZnO nanoribbons, $(ZnO)_2$NR, doped with Co atoms exhibit a piezomagnetic behavior. We find the formation of energetically stable zigzag chains of Co atoms along the edge sites of $(ZnO)_2$NR's, $Co_{Zn(chain)}$-$(ZnO)_2$NR. At the ground state, the antiferromagnetic and the ferromagnetic states are very close in energy, whereas upon longitudinal stretch, parallel to the nanoribbon growth direction, it becomes ferromagnetic. Further electronic structure calculations indicate that not only the magnetic state but also the electronic structure of $Co_{Zn(chain)}$-$(ZnO)_2$NR can be tuned by the mechanical stretch. In this case, we find that stretched NR's exhibit dispersive unpaired electronic states within the $(ZnO)_2$NR band gap.

DOI: 10.1103/PhysRevB.84.155309 PACS number(s): 73.20.At, 73.20.Hb

I. INTRODUCTION

Among the currently investigated semiconductor materials, zinc oxide (ZnO) can be considered to be one of the most studied. It is a quite malleable material, in the sense that different types of nanostructures can be synthesized by using ZnO,[1] viz., ZnO nanowires,[2] nanobelts,[3,4] planar sheets of ZnO,[5] and "exotic ZnO nanoribbons."[6,7] Such a degree of freedom is important, since we can tailor the electronic and the magnetic properties of ZnO nanostructures by controlling their geometrical characteristics in a suitable way. For instance, (i) the piezoelectric properties of ZnO nanowires allow us to convert mechanical energy to electric energy,[8] and (ii) there are experimental evidences of ferromagnetism in Mn-doped ZnO nanoparticles and thin films [9].

Room-temperature ferromagnetism in ZnO bulk doped with transition metals has been verified by several experimental groups,[10,11] however different explanations have been proposed.[12–14] For instance, in Ref. 14, the authors claim that the ferromagnetism in Co-doped ZnO is ruled by the presence of intrinsic defects (oxygen vacancies). On the other hand, there is experimental evidence of ferromagnetism in Co-doped ZnO nanostructures such as nanoparticles[15] and nanowires.[16] In those cases, the experimental results suggest that there is no need for the presence of intrinsic defects (like vacancies) in the Co-doped ZnO nanostructures. We may infer that the topology of the nanostructure plays an important role in the magnetic behavior of the Co-doped ZnO systems.[17] Indeed, recent theoretical investigations indicate that Co-doped single-layer ZnO sheets present a ferromagnetic coupling, while increasing the number of ZnO sheets (e.g., bilayered systems) causes such ferromagnetic coupling to be suppressed.[18]

As in graphene nanoribbons (NR's), the experimental realization of ZnO planar sheets[5] somewhat motivated a number of theoretical studies addressing the energetic stability and electronic properties,[19,20] as well as experimental investigations based on scanning tunneling microscopy images and electronic characterizations[7,21] of ZnO NR's. It is worth noting that planar structures for a few layers of ZnO were already predicted by Freeman *et al.*,[22] based upon *ab initio* total energy calculations. Nanoribbons can be considered to be a quasi-one-dimensional system, since the electronic states are confined perpendicularly to the ribbon growth direction (where the electronic confinement can be controlled by the width of the ribbon). Similar to surface states in bulk systems, we have to take into account their counterpart edge states in ribbon systems. For instance, magnetic properties have been predicted along the zigzag edges of graphene NR's,[23] and through the doping process (at the edge sites) we may have spin-polarized electron current along the NR's.[24] Magnetic behavior has also been proposed for zigzag ZnO NR's composed of a monolayer or a trilayer of ZnO. In contrast, such magnetic properties have been suppressed in bilayered ZnO NR's.[20] In addition, recent theoretical studies in single-layer zigzag ZnO NR's indicate that (i) edge passivated nanoribbons exhibit a half-metallic behavior,[25] and (ii) the magnetism along the edge sites can be tuned by application of an external electric field.[26] Those findings are important to the development of new nanodevices based on ZnO.

Motivated by the aforementioned findings, in this paper we investigate bilayer systems of zigzag NRs, $(ZnO)_2$NR's, doped with Co atoms. We find that zigzag $(ZnO)_2$NR represents an energetically stable configuration, when compared with single-layer ZnO nanostructures (sheet or ribbons). The formation of Co chains along the edge sites of the $(ZnO)_2$NR has been examined, where we find a piezomagnetic behavior. The magnetic state of such Co-doped $(ZnO)_2$NR can be tuned by applying a mechanical stretch along the NR growth direction. Further electronic structure investigations reveal the formation of unpaired electronic states, within the NR band gap, localized along the edge Co atoms of the stretched $Co_{Zn(chain)}$-$(ZnO)_2$NR's.

II. COMPUTATIONAL DETAILS

Our calculations were performed within the density functional theory (DFT) as implemented in the SIESTA code.[27] The local spin density approximation (LSDA)[28] approach has been used to calculate the exchange-correlation energy. The Kohn-Sham (KS) orbitals were described by linear combinations of numerical pseudoatomic orbitals using a split-valence double-zeta basis set including polarization functions.[29] The electron-ion interactions were calculated by using norm-conserving

pseudopotentials.[30] All the atomic positions were relaxed by using the conjugated gradient scheme, within a force convergence criterion of 10 meV/Å. The double-layer zigzag ZnO nanoribbon systems, $(ZnO)_2$NR's, have been simulated within the supercell approach. We have considered a 140 atom/supercell, where the nanoribbon structure is periodic along the growth direction ([0100] or z direction). Here, it is worth noting that the zigzag edges of the $(ZnO)_2$NR's correspond to the energetically stable $(10\bar{1}0)$ nonpolar surface of wurtzite ZnO nanowire growth along the [0001] direction.[31–35] As depicted in Fig. 1(a), we piled up five ZnO periodic units [shaded region in Fig. 1(a)] along the growth direction. In order to avoid interactions between the $(ZnO)_2$NR system and its image, due to the periodic boundary conditions, vacuum regions of ∼15 Å (x direction) and ∼10 Å (y direction) have been included, and the interaction between the opposite edges

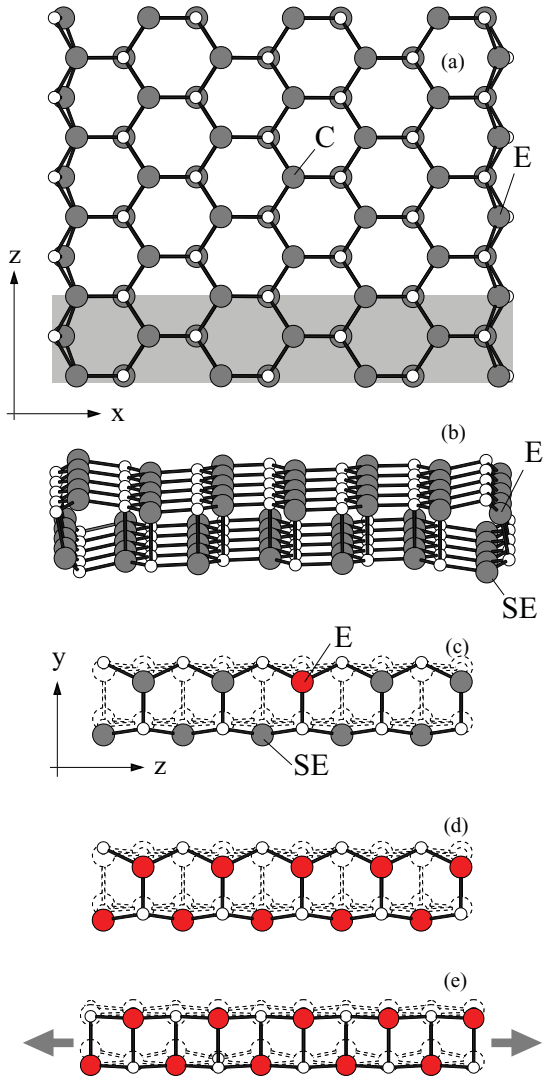

FIG. 1. (Color online) Structural model of $(ZnO)_2$NR: (a) top view and (b) side view. (c) Side view for a single Co_{Zn} atom occupying an edge (E) site, and (d) substitutional Co_{Zn} atoms forming an E-SE chain structure. (e) Co_{Zn} chain structure stretched along the NR growth direction, z. Filled red and gray circles represent the Co and Zn atoms, respectively, and empty (small) circles represent the O atoms.

of the $(ZnO)_2$NR's has been minimized by considering a NR width of 18 Å (x direction).

To check the validity of our results, with respect to the strong Coulombic repulsive interactions between the localized $3d$ orbitals (of Zn and Co atoms), we have performed additional DFT + U calculations as implemented in the Vienna Ab initio Simulation Package (VASP).[36] We choose $U_{3d} = 5$ and 2 eV for the Zn and Co $3d$ states, as proposed in Ref. 12 and applied for Co-doped ZnO. Here the electron-ion interactions were described through a fully relativistic pseudopotential within the projector augmented wave method (PAW),[37] and the KS orbitals were described by using a plane-wave basis set with an energy cutoff of 400 Ry.

We examine the relative energetic stability of $(ZnO)_2$NR, with respect to the other structural phases of ZnO, by comparing their formation energies (Ω). The formation energy difference ($\Delta\Omega$) can be written as

$$\Delta\Omega = \Omega[(ZnO)_2\text{NR}] - \Omega[\text{ZnO}X],$$

where $\Omega[(ZnO)_2\text{NR}]$ and $\Omega[\text{ZnO}X]$ represent the formation energies of the $(ZnO)_2$NR and a given structural phase X of ZnO, respectively. While the formation energy of neutral Co_{Zn}-doped $(ZnO)_2$NR is defined as

$$\Omega[\text{Co}_{\text{Zn}}] = E[\text{Co}_{\text{Zn}} - (\text{ZnO})_2\text{NR}] - E[(\text{ZnO})_2\text{NR}] - n_{\text{Zn}}\mu_{\text{Zn}} + n_{\text{Co}}\mu_{\text{Co}},$$

$E[\text{Co}_{\text{Zn}} - (\text{ZnO})_2\text{NR}]$ and $E[(\text{ZnO})_2\text{NR}]$ represent the calculated total energies of Co_{Zn}-doped and pristine $(ZnO)_2$NR's, respectively. n_{Zn} (n_{Co}) indicates the number of Zn (Co) atoms removed (added) from (to) $(ZnO)_2$NR, and μ_{Zn} (μ_{Co}) is its chemical potential.

III. RESULTS AND COMMENTS

Double-layer ZnO nanoribbon is a quite stable phase when compared with their counterpart monolayer systems, viz., ribbons and sheets. Indeed, we find that the $(ZnO)_2$NR is energetically more stable than single-layer ZnO nanoribbons by 1.623 eV per nanoribbon length, $\Delta\Omega = 1.623$ eV/Å. In this case, the energetic preference of $(ZnO)_2$NR's comes from the suppression of the dangling bonds present along the edge sites of a single-layer ZnO NR. In $(ZnO)_2$NR's, the edge Zn and O atoms are threefold coordinated due to the presence of underneath O and Zn (edge) atoms; see Figs. 1(a) and 1(b). At the equilibrium geometry, the inner sites of $(ZnO)_2$NR exhibit a quasiplanar (nonpolar) structure, where the Zn and O atoms present a height difference (u) smaller than 0.07 Å, in agreement with the experimental results, $u = 0.12 \pm 0.10$ Å, for depolarized planar bilayer sheets of ZnO.[5] In contrast, near the edge sites of the NR, we find u between 0.30 and 0.76 Å, which is due to the formation of (edge) Zn-O bonds. On the other hand, different from the (single-layer) ribbon systems, there are no dangling bonds in two-dimensional monolayer sheets of ZnO, however we find $\Delta\Omega = 0.544$ eV/Å. That is, $(ZnO)_2$NR's are energetically more stable than single-layer ZnO sheets. In spite of its energetic stability, unfortunately, $(ZnO)_2$NR does not present the magnetic properties predicted for monolayer and trilayer systems of zigzag ZnO NRs.[20,25,26]

$(ZnO)_2$NR exhibits a semiconducting character. We obtained an energy band gap of 1.7 eV, being slightly larger than the one obtained for two-dimensional ZnO bilayer sheets. This is due to the electronic confinement perpendicular to the ribbon growth direction. By including the on-site Coulombic interaction (U_{3d} for Zn), we obtained an energy band gap of 2.02 eV for the $(ZnO)_2$NR system.[38] The magnetic properties in ZnO structures can be tailored through suitable doping processes. Indeed, previous theoretical investigations indicate that substitutional Co_{Zn} atoms present a ferromagnetic coupling in monolayer ZnO sheets, while it becomes antiferromagnetic in double-layered ZnO sheets.[18] We next examine the energetic and magnetic properties of Co_{Zn} atoms in $(ZnO)_2$NR's.

Initially, we perform a total energy search for the most likely configuration for a substitutional Co_{Zn} atom in $(ZnO)_2$NR. We have considered Co atoms occupying the Zn sites as depicted in Figs. 1(a)–1(c). We find that Co_{Zn} at the edge site (E), $Co_{Zn(E)}$ configuration, is energetically more favorable by 0.587 and 0.063 eV when compared with Co_{Zn} occupying the central (C) and subedge (SE) sites, respectively. The latter total energy difference indicates that $Co_{Zn(SE)}$ is also a quite likely configuration. The semiconducting character of $(ZnO)_2$NR's has been maintained, with an energy gap of 1.7 eV. Indeed, the valence-band maximum (VBM) and the conduction-band minimum (CBM) are weakly perturbed due to the presence of Co_{Zn} impurities. Figure 2 presents the total density of states (DOS) of $Co_{Zn(E)}$-doped $(ZnO)_2$NR, and the projected density

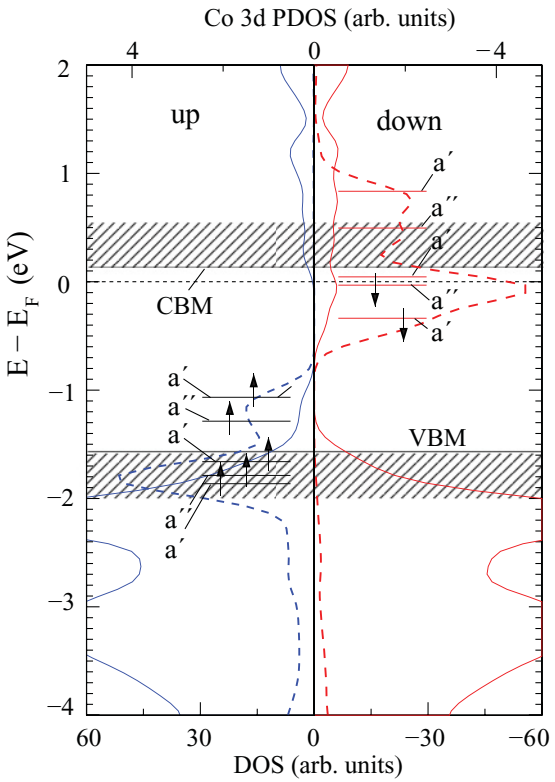

FIG. 2. (Color online) Total density of states (solid lines), projected density of states (dashed lines), and the respective energy levels of Co 3*d* for the $Co_{Zn(E)}$-doped $(ZnO)_2$NR. We have considered a Gaussian (broadening) width of 0.2 eV for the DOS and PDOS diagrams.

of states (PDOS) of $Co_{Zn(E)}$ 3*d* orbitals. The occupied majority (spin-up) Co 3*d* orbitals are localized within an energy interval of 1–2 eV below the Fermi level (E_F), where the two highest occupied spin-up states lie at the band gap of $(ZnO)_2$NR, while the occupied minority (spin-down) Co 3*d* states are localized within $E_F - 1$ eV. We find a net magnetic moment of $3.0\mu_B$, mostly ruled by the Co 3*d* orbitals, for a single Co_{Zn} at the edge site of $(ZnO)_2$NR. The highest occupied and the lowest unoccupied minority (spin-down) states of Co 3*d* are also localized within the $(ZnO)_2$NR band gap. As we verified above, by including the repulsive interaction between the Zn 3*d* electrons (DFT + U calculations), the band gap of $(ZnO)_2$NR increases to 2.02 eV. Similarly, by including $U_{3d} = 2$ eV (5 eV) for the Co (Zn) 3*d* orbitals, we find that the lowest unoccupied (spin-down) state moves upward with respect to the Fermi level, becoming resonant within the conduction band of the $(ZnO)_2$NR host, around CBM + 0.5 eV. In contrast, the energy positions, with respect to the Fermi level, of the highest occupied spin-down Co 3*d* orbitals are almost the same when compared with the LSDA results. Here we find a net magnetization of $2.9\mu_B$, and thus further support for our LSDA results for the Co_{Zn}-doped $(ZnO)_2$NR. It is worth pointing out that, due to the electronic confinement in NR systems, the highest occupied Co 3*d* (impurity) orbital does not lie within the conduction band of $(ZnO)_2$NR, thus we do not face the "false occupation" problem verified in DFT-GGA/LDA calculations for 3*d* impurities embedded in ZnO bulk systems.[12–14,39] Additional calculations indicate that $Co_{Zn(SE)}$ exhibits a similar electronic structure when compared with $Co_{Zn(E)}$ in $(ZnO)_2$NR. For instance, the energy positions of the Co 3*d* orbitals are practically the same for $Co_{Zn(E)}$ and $Co_{Zn(SE)}$.

The Co_{Zn}-doped $(ZnO)_2$NR, with the Co_{Zn} at the E or SE sites, belongs to the C_s point group. In this case, the Co 3*d* orbital splits in nondegenerated a' and a'' states, as depicted in Fig. 2. Based upon the phenomenological band-structure model proposed by Dalpian *et al.*,[40] we examine the energy gain for the ferromagnetic (FM) and antiferromagnetic (AFM) configurations in Co_{Zn}-doped $(ZnO)_2$NR's. Within this approach, we considered only the electronic coupling between Co 3*d* orbitals. For the FM system, there is no energy gain due to the electronic interaction between the occupied majority states. In contrast, the electronic interactions between the occupied and unoccupied minority states give rise to a net energy gain. Meanwhile, for the AFM system the energy gain is ruled by electronic interactions between the majority and minority 3*d* states. Both systems (FM and AFM) present a net energy gain, however the energy gain of the FM system is expected to be larger when compared with that of the AFM system. As indicated in Fig. 2, the energy gain of the AFM system comes from electronic interactions between majority (occupied) and minority (unoccupied) states distant in energy by more than 1 eV, whereas for the FM system, the energy gain comes from electronic interactions between minority occupied and unoccupied states distant in energy by less than 0.2 eV.

Indeed, placing two Co_{Zn} in $(ZnO)_2$NR, we find an energetic preference for the FM configuration. Based upon total energy results, we examine two plausible geometries for the substitutional Co_{Zn} atoms. We find that one Co_{Zn} at the E site and another at the nearest-neighbor SE site, $Co_{Zn(E)}$-$Co_{Zn(SE)}$, represents the most likely configurations, followed by

the $Co_{Zn(E)}$-$Co_{Zn(E)}$ configuration (two Co_{Zn} atoms occupying nearest-neighbor E sites). We verify that the FM state is more stable than the AFM state by 0.370 and 0.071 eV for $Co_{Zn(E)}$-$Co_{Zn(SE)}$ and $Co_{Zn(E)}$-$Co_{Zn(E)}$ structures, respectively. At the equilibrium geometry, the Co-Co bond distance, for $Co_{Zn(E)}$-$Co_{Zn(SE)}$ in $(ZnO)_2$NR, is 2.37 and 2.39 Å for the FM and AFM states, respectively.

By increasing the presence of substitutional Co atoms, we find the formation of energetically stable zigzag chain of Co_{Zn} atoms lying on the E and SE sites of $(ZnO)_2$NR, $Co_{Zn(chain)}$-$(ZnO)_2$NR, depicted in Fig. 1(d). Comparing the formation energies of Co_{Zn} ($\Omega[Co_{Zn}]$ in Sec. II) forming a $Co_{Zn(E)}$-$Co_{Zn(E)}$ isolated pair, and Co_{Zn} forming a $Co_{Zn(chain)}$ structure along the edge sites of $(ZnO)_2$NR, we find that the latter is energetically more favorable by 0.29 eV/Co atom. However, the energetic preference for the FM state is somewhat suppressed in $Co_{Zn(chain)}$-$(ZnO)_2$NR. In fact, we find an energetic preference for the AFM configuration by 0.052 eV, $\Delta E_{AFM-FM} = -0.052$ eV. On the other hand, due to the high concentration of Co_{Zn} atoms along edge sites of the ribbon, the (periodic) length of $Co_{Zn(chain)}$-$(ZnO)_2$NR (l) increases by 2.5% in comparison with that of pristine $(ZnO)_2$NR (l_0). That is, at the ground state, $l/l_0 = 1.025$ for the $Co_{Zn(chain)}$-$(ZnO)_2$NR system. In this case, the (slight) energetic preference for the AFM state has been maintained, $\Delta E_{AFM-FM} = -0.013$ eV; see Figs. 3(a) and 3(b). In contrast, for $l/l_0 = 1.05$, the FM configuration becomes energetically more favorable, $\Delta E_{AFM-FM} = 0.026$ eV. The energetic preference for the FM configuration is strengthened upon further stretch of the $Co_{Zn(chain)}$-$(ZnO)_2$NR structure. For $l/l_0 = 1.10$ and 1.125, we obtained $\Delta E_{AFM-FM} = 0.064$ and 0.119 eV, and a net magnetization of $6.0\mu_B$. Thus, we can infer that the magnetic state of $(ZnO)_2$NR, decorated with a Co_{Zn} chain attached along the E and SE sites, can be tuned through a mechanical strain along the NR growth direction. $Co_{Zn(chain)}$-$(ZnO)_2$NR structures exhibit a piezomagnetic behavior. We next check the validity of the proposed piezomagnetic behavior through additional calculations of ΔE_{AFM-FM}, as a function of the longitudinal stretch, within the DFT + U approach described in Sec. II. In this case, (i) the ground-state configuration occurs for $l/l_0 = 1.025$, with $\Delta E_{AFM-FM} \approx 0$, Fig. 3(c). (ii) The AFM state becomes energetically more favorable for compressed systems, namely, for $l/l_0 = 0.975$ and 0.95, we find $\Delta E_{AFM-FM} = -0.007$ and -0.037 eV, respectively. (iii) Stretching the $Co_{Zn(chain)}$-$(ZnO)_2$NR, we find that the FM state becomes energetically more favorable, with $\Delta E_{AFM-FM} = 0.05$ and 0.12 eV for $l/l_0 = 1.05$ and 1.10, respectively, with a net magnetization of $5.8\mu_B$ for both systems, in agreement with the LSDA calculation. Those results indicate that the piezomagnetic behavior of $Co_{Zn(chain)}$-$(ZnO)_2$NR's has been maintained upon the inclusion of Coulombic repulsive interactions between 3d electrons of Zn and Co atoms.

The magnetic properties of $Co_{Zn(chain)}$-$(ZnO)_2$NR are ruled by Co_{Zn} 3d orbitals. In Fig. 4, we present our DFT + U results for the electronic structure calculations.[41] For the AFM $Co_{Zn(chain)}$-$(ZnO)_2$NR, with $l/l_0 = 1.025$, the electronic distribution of Co 3d orbitals is practically the same for both spin-up and -down channels, and the system presents a semiconducting character, with an energy gap of 1.2 eV; see Fig. 4(a). For the FM system ($l/l_0 = 1.10$), Figs. 4(b) and 4(c), the number of occupied spin-down orbitals is reduced, mainly within the valence band of the $Co_{Zn(chain)}$-$(ZnO)_2$NR [Fig. 4(b)], where we find a net magnetic moment of $5.8\mu_B$, localized along the Co_{Zn} chain. In addition, along the $Co_{Zn(chain)}$ structure the electronic interactions among the Co_{Zn} atoms increase, giving rise to dispersive (spin-down) electronic states within the $(ZnO)_2$NR band gap, see Fig. 4(c), while the highest occupied spin-up states are localized within the valence band of the Co-doped $(ZnO)_2$NR. Similar electronic band structure has been verified for the $l/l_0 = 1.125$ FM system. In this case, we can infer a spin-polarized current along the stretched systems

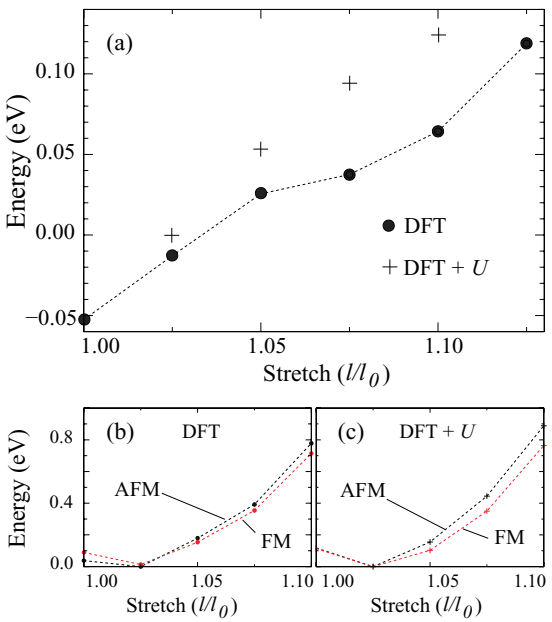

FIG. 3. (Color online) (a) Total energies difference between the AFM and FM states, $\Delta E_{AFM-FM} = E_{AFM} - E_{FM}$, as a function of the longitudinal stretch (l/l_0) along the z direction. Total energy as a function of l/l_0 (b) DFT, and (c) DFT + U calculations.

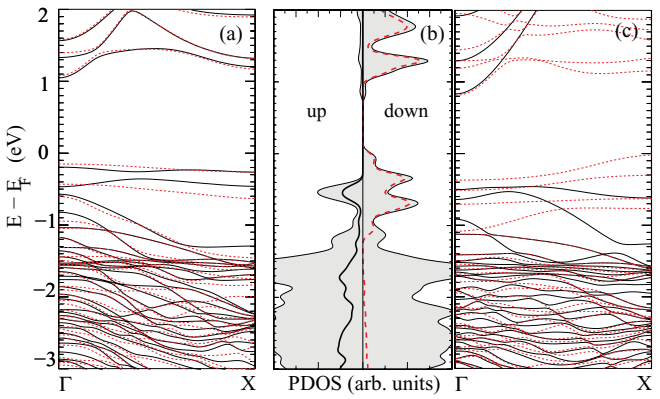

FIG. 4. (Color online) DFT + U results for (a) electronic band structure for the AFM $Co_{Zn(chain)}$-$(ZnO)_2$NR, with $l/l_0 = 1.025$. (b) Projected electronic density of states of the stretched $Co_{Zn(chain)}$-$(ZnO)_2$NR systems, FM state with $l/l_0 = 1.10$, shaded regions indicate the total density of states, and solid (dashed) lines indicate the spin-up (-down) Co 3d projected density of states. (c) Electronic band structure along the ΓX direction (i.e., parallel to the NR growth direction) for the FM state with $l/l_0 = 1.10$.

mediated by a *p*-type doping. Thus, not only the magnetization but also the electronic band structure can be tuned by stretching the $Co_{Zn(chain)}$-$(ZnO)_2$NR system.

IV. CONCLUSIONS

In conclusion, we show that Co_{Zn}-doped $(ZnO)_2$NR's exhibit a piezomagnetic behavior. The magnetic state of $Co_{Zn(chain)}$-$(ZnO)_2$NR can be tuned by applying a mechanical stretch along the nanoribbon growth direction. Initially, we find that there is an energetic preference for Co_{Zn} occupying the edge sites of $(ZnO)_2$NR's, giving rise to Co_{Zn} dimers. Those Co_{Zn} dimers exhibit a FM ground-state configuration. However, such an FM state is suppressed upon the increase of Co_{Zn} concentration. We find the formation of energetically stable zigzag chains of Co_{Zn} atoms along the edge sites of $(ZnO)_2$NR's, $Co_{Zn(chain)}$-$(ZnO)_2$NR. In this case, the FM and AFM states along the $Co_{Zn(chain)}$ structure are very close in energy. Further total energy investigations reveal that the magnetic and the electronic properties of $Co_{Zn(chain)}$-$(ZnO)_2$NR structures can be tuned by applying a mechanical stretch along the $(ZnO)_2$NR growth direction. In this case, the $Co_{Zn(chain)}$-$(ZnO)_2$NR system becomes FM upon a longitudinal stretch.

ACKNOWLEDGMENTS

The authors acknowledge financial support from the Brazilian agencies CNPq/INCT, FAPEMIG, FAPESP, and computational support from CENAPAD/SP.

*hiroki@infis.ufu.br

[1] M. Ahmad and J. Zhu, J. Mater. Chem. **21**, 599 (2011).
[2] M. H. Huang, S. Mao, H. Feick, H. Yan, Y. Wu, H. Kind, E. Weber, R. Russo, and P. Yang, Science **292**, 1897 (2001).
[3] W. Z. Pan, Z. Dai, and Z. L. Wang, Science **291**, 1947 (2001).
[4] X. Wang, Y. Ding, C. J. Summers, and Z. L. Wang, J. Phys. Chem. B **108**, 8773 (2004).
[5] C. Tusche, H. L. Meyerheim, and J. Kirschner, Phys. Rev. Lett. **99**, 026102 (2007).
[6] L. Wang, K. Chen, and L. Dong, J. Phys. Chem. C **114**, 17358 (2010).
[7] T. G. G. Maffeis, M. W. Penny, J. D. W. Garbut, and S. P. Wilks, Phys. Status Solidi **207**, 282 (2010).
[8] Z. L. Wang and S. J. Song, Science **312**, 242 (2006).
[9] N. S. Norberg, K. R. Kittilstved, J. E. Amonette, R. K. Kukkadapu, D. A. Schwartz, and D. R. Gamelin, J. Am. Chem. Soc. **126**, 9387 (2004).
[10] K. Ueda, H. Tabata, and T. Kawai, Appl. Phys. Lett. **79**, 988 (2001).
[11] M. Venkatesan, C. B. Fitzgerald, J. G. Lunney, and J. M. D. Coey, Phys. Rev. Lett. **93**, 177206 (2004).
[12] A. Walsh, J. L. F. Silva, and S.-H. Wei, Phys. Rev. Lett. **100**, 256401 (2008).
[13] S. Lany, H. Raebiger, and A. Zunger, Phys. Rev. B **77**, 241201 (2008).
[14] C. D. Pemmaraju, R. Hanafin, T. Archer, H. B. Braun, and S. Sanvito, Phys. Rev. B **78**, 054428 (2008).
[15] Z. H. Zhang, X. Wang, J. B. Xu, S. Muller, C. Ronning, and Q. Li, Nat. Nanotechnol. **4**, 523 (2009).
[16] X. Wang, F. Song, Q. Chen, T. Wang, J. Wang, P. Liu, M. Shen, J. Wan, G. Wang, and J. B. Xu, J. Am. Chem. Soc. **132**, 6492 (2010).
[17] R. Podila *et al.*, Nano Lett. **10**, 1383 (2010).
[18] T. M. Schmidt, R. H. Miwa, and A. Fazzio, Phys. Rev. B **81**, 195413 (2010).
[19] A. R. Botello-Mendéz, M. T. Martínez-Martínez, F. Lópes-Urías, M. Terrones, and H. Terrones, Chem. Phys. Lett. **448**, 258 (2007).
[20] A. R. Botello-Mendéz, F. Lópes-Urías, M. Terrones, and H. Terrones, Nano Lett. **8**, 1562 (2008).
[21] H. Y. Shih, Y. T. Chen, N. H. Huang, C. M. Wei, and Y. F. Chen, J. Appl. Phys. **109**, 103523 (2011).
[22] C. L. Freeman, F. Claeyssens, N. L. Allan, and J. H. Harding, Phys. Rev. Lett. **96**, 066102 (2006).
[23] H. Lee, Y.-W. Son, N. Park, S. Han, and J. Yu, Phys. Rev. B **72**, 174431 (2005).
[24] T. B. Martins, R. H. Miwa, A. J. R. da Silva, and A. Fazzio, Phys. Rev. Lett. **98**, 196803 (2007).
[25] Q. Chen, L. Zhu, and J. Wang, Appl. Phys. Lett. **95**, 113116 (2009).
[26] L. Kou, C. Li, Z. Zhang, and W. Guo, ACS Nano **4**, 2124 (2010).
[27] J. M. Soler, E. Artacho, J. D. Gale, A. García, J. Junquera, P. Ordejón, and D. Sánchez-Portal, J. Phys. Condens. Matter **14**, 2745 (2002).
[28] D. M. Ceperley and B. J. Alder, Phys. Rev. Lett. **45**, 566 (1980).
[29] Within the SIESTA code, the cutoff radius of the basis set (pseudoatomic orbitals) can be tuned by a single parameter, *energy shift*. For lower *energy shift* we have larger cutoff radii for the atomic orbitals, that is, the basis set has been improved. In the present work, we have considered an energy shift of 0.10 eV to determine the radius cutoff of the pseudoatomic orbitals. Here we verify the convergence of our total energy results for an *energy shift* of 0.05 eV.
[30] N. Troullier and J. L. Martins, Phys. Rev. B **43**, 1993 (1991).
[31] C. Li, W. Guo, Y. Kong, and H. Gao, Phys. Rev. B **76**, 035322 (2007).
[32] X. Shen, P. B. Allen, J. T. Muckerman, J. D. Davenport, and J.-C. Zheng, Nano Lett. **7**, 2267 (2007).
[33] L. Zhang and H. Huang, Appl. Phys. Lett. **90**, 23115 (2007).
[34] H. Xu, A. L. Rosa, T. Frauenheim, R. Q. Zhang, and S. T. Lee, Appl. Phys. Lett. **91**, 031914 (2007).
[35] T. M. Schmidt and R. H. Miwa, Nanotech. **20**, 215202 (2009).
[36] G. Kresse and J. Furthmüller, Phys. Rev. B **54**, 11169 (1996).
[37] P. E. Blöchl, Phys. Rev. B **50**, 17953 (1994).
[38] For the ZnO bulk phase, the energy band gap increases by 0.55 eV, 0.66 $\rightarrow$1.17 eV, within the DFT + U calculation.
[39] A. Zunger, S. Lany, and H. Raebiger, Physics **3**, 53 (2010).
[40] G. M. Dalpian, S.-H. Wei, X. Gong, A. J. da Silva, and A. Fazzio, Solid State Commun. **138**, 353 (2006).
[41] Within the LSDA approach, we find metallic spin-down channels for the FM Co-doped ZnO nanoribbon, however, by inclusion of the Hubbard U for the Zn and Co 3d orbitals, DFT + U calculations, we verify that those partially occupied metallic states are suppressed.